

## Polarization of light scattered by particles on silicon wafers

Lipiin Sung,<sup>a,b</sup> George W. Mulholland,<sup>a</sup> and Thomas A. Germer<sup>a</sup>

<sup>a</sup>National Institute of Standards and Technology, Gaithersburg, MD 20899

<sup>b</sup>University of Maryland, College Park, MD 20742

### ABSTRACT

Bidirectional ellipsometry has been developed as a technique for distinguishing among various scattering features near surfaces. Employing incident light with fixed polarization, the technique measures the principal angle of polarization and the degree of linear polarization of light scattered into directions out of the plane of incidence. This technique has been previously shown to be successful at distinguishing between subsurface defects and microroughness. Theoretical models have predicted that the polarization of light scattered by particles should also be different than that scattered by subsurface defects and microroughness. In this paper, experimental results will be presented which show good agreement with these models for a range of sizes of polystyrene latex spheres on silicon wafers. The results demonstrate that the polarization of light scattered by particles can be used to determine the size of particulate contaminants on silicon wafers and other smooth surfaces. The model calculations, based on different degrees of approximation, demonstrate that the mean distance of a particle from the surface is the primary determinant of the scattered light polarization for small scattering angles.

Keywords: bidirectional ellipsometry, particles, polarimetry, polystyrene latex spheres, scattered light, surfaces.

### 1. INTRODUCTION

A major concern to the semiconductor industry is the detection and characterization of particles and defects on silicon wafers. Instruments based upon light scattering satisfy many of the requirements of the industry, such as high throughput rate and high sensitivity. However, scattered light may arise from a number of different sources, such as surface roughness, surface residue, particulate contamination, and subsurface defects. Recently, Germer *et al.*<sup>1-4</sup> have demonstrated experimentally and theoretically that the polarization of scattered light can be used to distinguish among various types of light scattering features near surfaces. Using the unique polarization properties of each scatter source, one can separate the contribution from the various sources of scattering, and improve the ability of optical inspection tools to detect particulate contamination and subsurface defects over a background dominated by substrate microroughness.

In this paper, we present a model system containing accurately-sized polystyrene latex (PSL) spheres on a silicon surface to test theoretical models for particles above a surface. These models predict that the angular dependence of the polarization depends upon particle size. This effect allows the size of particles to be determined. Using bidirectional ellipsometry, we measure the principal angle of polarization and the degree of linear polarization of light scattered from the model system into directions out of the plane of incidence. The experimental results of the model system having different particle sizes show good agreement with the theoretical predictions.

In Sec. 2, we review the theoretical models for light scattered from a system containing spheres above a smooth surface with different degrees of approximation. In Sec. 3, we briefly describe the sample preparation and

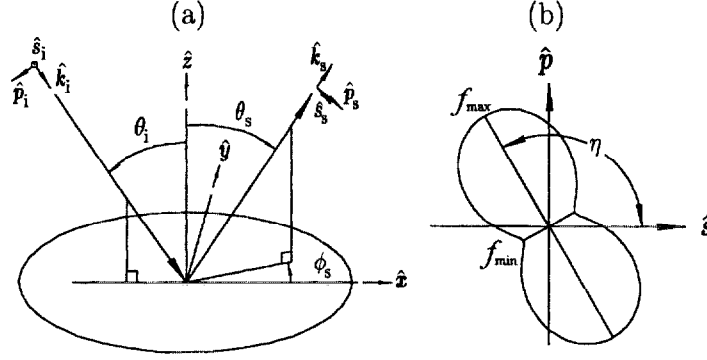


**Figure 1** (a) The sample coordinate system used in this paper; and (b) a schematic of the intensity distribution  $f$  measured by a rotating linear-polarization-sensitive detector, defining the bidirectional ellipsometry parameters,  $\eta$  and  $P_L = (f_{\max} - f_{\min})/(f_{\max} + f_{\min})$ .

the experimental procedure employed for these measurements. In Sec. 4, we present the experiment results and compare them to the theory. Finally, the results are summarized in Sec. 5.

## 2. THEORY

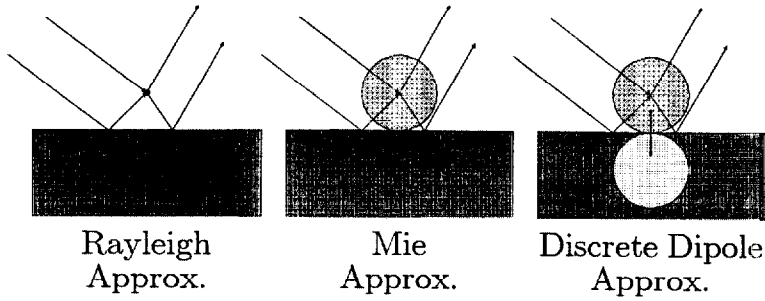
Theories describing the light scattered by a spherical particle of diameter  $D$  and complex refractive index  $n_{\text{sph}}$  above a smooth surface of complex refractive index  $n_s$  have been developed elsewhere.<sup>1,5-13</sup> In order to compare to the experimental results from bidirectional ellipsometry directly, we use a sample coordinate system, shown in Fig. 1(a), to describe the angular dependence and the polarization of the scattered field. Plane wave polarized light of wavelength  $\lambda$  irradiates the surface at an incident angle  $\theta_i$  in the plane defined by  $\hat{x}$  and  $\hat{z}$ . We measure the polarization of light scattered into a direction defined by a polar angle  $\theta_s$  and an out-of-plane angle  $\phi_s$ . Unit vectors  $\hat{k}_i$  and  $\hat{k}_s$  describe the directions of propagation of the incident and scattered light, respectively. The polarization of the incident field is described by the components of the electric field along the  $\hat{s}_i$  and  $\hat{p}_i$  directions, where  $\hat{s}_i$  is a unit vector perpendicular to both  $\hat{k}_i$  and  $\hat{z}$ , and  $\hat{p}_i = \hat{k}_i \times \hat{s}_i$ . Likewise, the polarization of the scattered field in a particular direction is described by the components of the electric field along the  $\hat{s}_s$  and  $\hat{p}_s$  unit vectors, defined in an analogous manner as  $\hat{s}_i$ , and  $\hat{p}_i$ . We say that incident light is  $p$ -polarized ( $s$ -polarized) when it is linearly polarized with its electric field in the  $\hat{p}_i$  ( $\hat{s}_i$ ) direction.

Figure 1(b), schematically showing the signal as one rotates a polarizer in front of a detector, illustrates the definition of the bidirectional ellipsometry parameters,  $\eta$  and  $P_L$ . The degree of linear polarization  $P_L$  is given by

$$P_L = (f_{\max} - f_{\min})/(f_{\max} + f_{\min}). \quad (1)$$

These parameters are easily derived from the Mueller matrix.<sup>2</sup> For linearly polarized light,  $P_L = 1$ , and for unpolarized light or circularly polarized light,  $P_L = 0$ . The angle  $\eta^{(p)}$  is the angle that the principle axis of the polarization ellipse makes with respect to the  $\hat{s}$  direction when  $p$ -polarized light is incident on the sample, and the corresponding degree of linear polarization is  $P_L^{(p)}$ .

In this section, we briefly review three approximations, schematically illustrated in Fig. 2, for calculating the angular dependence and polarization of light scattered by a particle above a smooth surface. In the Rayleigh approximation,<sup>1,11-13</sup> which is only valid if the particle size is much smaller than the wavelength of the light, the scatterer is treated as a point polarizable dipole. The finite size of the particle and particle-substrate interaction are ignored in this approximation. The key parameter in this approximation is the mean distance  $d = D/2$  of



**Figure 2** Schematic diagram illustrating three theoretical approximations for scattering from a spherical particle above a smooth surface.

the particle from the surface. The diameters of the PSL spheres we used in this study are sufficiently large that the angular dependence and polarization of light scattered from an isolated sphere is not entirely Rayleigh-like. In the Mie approximation, we include the diffraction of the scattered field by a homogeneous sphere, using the exact Mie solution<sup>5,6</sup> for a sphere in free space.<sup>9,11,12</sup>

In both Rayleigh and Mie approximations, we neglect the interaction between the particle and its image in the substrate (i.e. the particle-substrate interaction). To account for this interaction, a discrete-dipole approximation (DDA) is used. In this model, an object is built out of a large number of interacting dipoles. The near field interactions between each dipole directly and through their reflections in the surface are included in the calculation [See Fig. 2]. A complete description of the code used to perform these calculations is given in a number of publications.<sup>10,14-16</sup>

In all the calculations performed in this study, we assume indices of refraction appropriate for  $\lambda = 532$  nm:  $n_{\text{sph}} = 1.59$  and  $n_s = 4.05 + 0.05 i$ . Fig. 3 compares the predictions of the three models for the bidirectional ellipsometry parameters for four different particle diameters. The interaction between particles are neglected in all these calculations. Note that the effect of the finite size of the particle and the interaction between sphere and substrate become noticeable as the particle diameter increases. However, the predictions for  $\eta^{(p)}$  at small  $\phi_s$  are relatively independent of the model. This finding indicates that the strongest determining factor of the parameter  $\eta^{(p)}$  at small  $\phi_s$  is the mean distance of the particle from the surface and not the index of refraction of the particle. Fig. 4(a) shows the angular dependence of  $\eta^{(p)}$  for different particle sizes using the DDA model. It is evident that  $\eta^{(p)}$  have a unique angular dependence for each particle size.

One can relate the slope of the  $\eta^{(p)}$  vs.  $\phi_s$  curves near  $\phi_s = 0$  to the particle size. Fig. 4(b) shows the slope,  $-\delta\eta^{(p)}/\delta\phi_s$ , evaluated at  $\phi_s = 0$ , as a function of the diameter of the particle for the three different approximations. All three models predict similar behaviors in the displayed region, and converge to each other for small diameters. Again this result implies that only measurements extended to large out-of-plane scattering angles may provide information about the particle-substrate interaction, the particle shape, or the particle material. Experimental data obtained from three particle sizes are also shown in Fig. 4(b) and will be discussed later in the text.

Theoretically, we demonstrate that the polarization of light scattered by particles can be used to determine the size of particles on a smooth surface. In all approximations, the particle size can be estimated by the slope of  $\eta^{(p)}$  in the small  $\phi_s$  region. However, to determine the size more accurately and to obtain the information about particle-substrate interaction, the particle shape, or the particle material, we need to measure the bidirectional ellipsometry parameters for a wide range of  $\phi_s$ . Since the DDA model is the best approximation of the three, we use it for the remainder of the paper to compare to the experimental data.

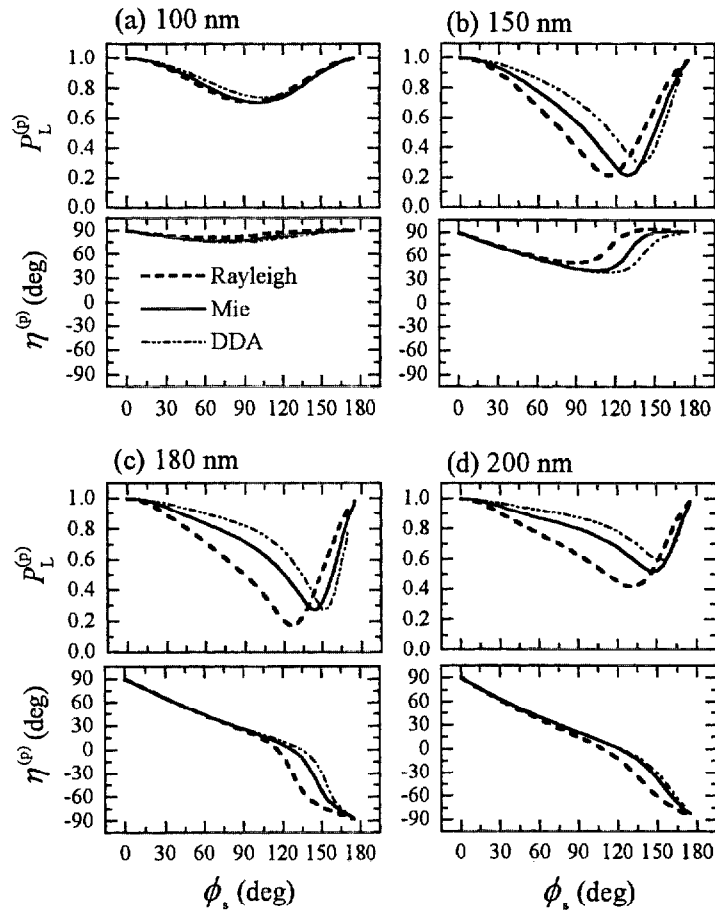


**Figure 3** Results of bidirectional ellipsometry calculations using three approximations for light scattering from four diameters of PSL spheres above a smooth silicon surface at  $\lambda = 532$  nm. The incident and scattering polar angles are  $\theta_i = \theta_s = 45^\circ$ .

### 3. EXPERIMENTAL DETAILS

In order to test the model for light scattering from dielectric spheres on a silicon surface, we use a range of accurately-sized polystyrene latex (PSL) spheres deposited on the bare silicon substrate for the simulation of particulate contamination. In this section, we describe the sample preparations and the bidirectional ellipsometry measurements.

#### 3.1 Sample Preparations

A low-pressure impactor connecting to a particle generation/classification system is used to deposit monodisperse particles onto silicon wafers. The particle generation/classification system consists of an aerosol generation system (nebulizer), a differential mobility analyzer (DMA) for size selection, and a condensation nucleus counter

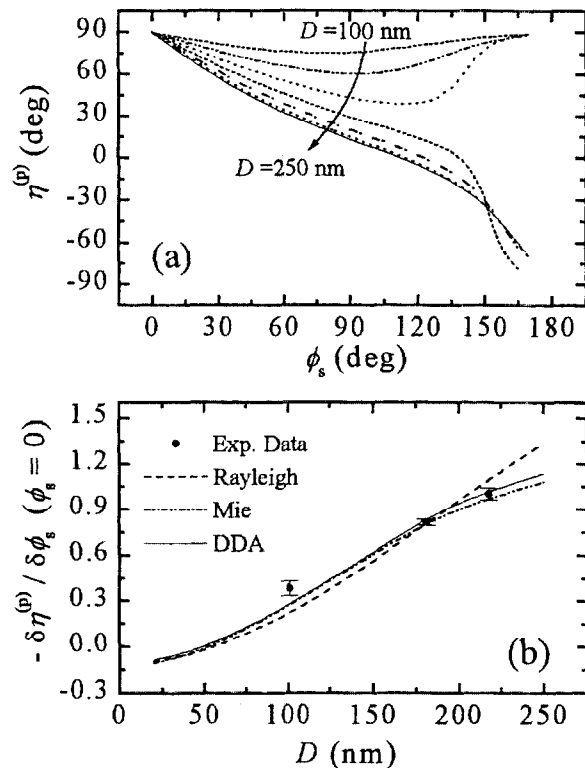


**Figure 4** (a) DDA model predictions for  $\eta^{(p)}$  as a function of  $\phi_s$  for various particle diameters, and for  $\theta_i = \theta_s = 45^\circ$ . The value of  $D$  increases monotonically by 25 nm per curve from 100 nm (top curve) to 250 nm (bottom curve). (b) The initial slope,  $-\delta \eta^{(p)} / \delta \phi_s$ , evaluated at  $\phi_s = 0$ , as a function of the diameter of the particle for three theoretical approximations with the experimental results for three different particle sizes.

for monitoring the aerosol concentration. Details of design and evaluation of the low-pressure impactor and the particle generation/classification system are described in detail elsewhere.<sup>17-19</sup>

Polystyrene latex (PSL) spheres ranging from 100 nm to 300 nm in diameter have been chosen and deposited on the bare wafers. Results for three diameters of PSL spheres are presented in this paper. One is the 100 nm NIST SRM1963 particle standard, and the other two PSL sphere solutions were obtained from Duke Scientific Corporation,<sup>20</sup> which specified nominal diameters of 183 nm and 220 nm. By controlling the concentration of PSL solution, the flow rate of the aerosol and the sheath air, and the DMA voltage, the deposition rate of particles through the low-pressure impactor can be selected.<sup>18,19</sup>

Prior to particle deposition, the clean wafers appeared featureless under a microscope. After deposition, the samples were examined using a dark field reflection optical microscope (1000 × magnification) to estimate the density of the spheres on the wafers. For the larger two particle sizes, the number density is estimated to be about  $0.03 \mu\text{m}^{-2}$  in the illuminated sample regions. Less than 2 % of the particles were doublets (two-touching spheres) on the samples containing 183 nm and 220 nm spheres, and the particles are well-separated from each other. The dark field optical microscopy results were inconclusive for the 100 nm particles. A field emission

scanning electron microscope operated at 5 keV and  $20000\times$  magnification indicated about 10 % of the particles were doublets and that the number density was about  $0.2\ \mu\text{m}^{-2}$ , which is about 7 times higher than for the other samples. The light scattered from doublets may affect the results of bidirectional ellipsometric measurements, which we will discuss in Sec. 4.

The mean particle size of the monodisperse PSL aerosol is measured by the differential mobility analyzer (DMA) using the 100 nm spheres to calibrate the flow of the classifier. The actual sizes of the three particles are  $100.7 \pm 1.0$  nm,  $180.0 \pm 6.0$  nm and  $217.7 \pm 3.4$  nm<sup>19,21–23</sup> with a polydispersity less than 2 %. An approximate particle size of 186 nm<sup>21</sup> was obtained for the middle particle size in a series of screening measurements which involved 22 samples including the 217.7 nm particles. Subsequent more accurate measurements<sup>22</sup> indicated that the screening measurement of 186 nm was an overestimate by about 2.5 %. The corrected particle size is 181 nm with an estimated uncertainty interval of  $\pm 6$  nm at 95 % confidence level. We use these actual particle sizes for the corresponding diameter in the DDA model for the comparison between the theory and experiment.

### 3.2 Bidirectional Ellipsometric Measurements

The Goniometric Optical Scatter Instrument (GOSI), which was used to perform the measurements described in this paper, is described in detail elsewhere.<sup>4,24</sup> Briefly, laser light of wavelength  $\lambda = 532$  nm is incident onto a sample at an angle  $\theta_i$ , and light scattered into the direction defined by the angles  $\{\theta_s, \phi_s\}$  is collected [see Fig. 1(a)]. The polarization state of the incident light is selected with a fixed linear polarizer followed by a rotating  $\lambda/2$  linear retarder. The polarization state of the scattered light is analyzed with a rotating  $\lambda/2$  linear retarder followed by a fixed linear polarizer. Although a bidirectional ellipsometric measurement can be carried out by fixing the incident light polarization while rotating the detection polarization optics, all of the measurements described in this paper were made by measuring the  $3 \times 3$  upper left-hand corner of the Mueller matrix (non-handed Mueller matrix) using a  $(\omega, 4\omega)$  scheme,<sup>25</sup> whereby the receiving retarder is rotated at four times the rate of the incident light retarder. The signal is measured at 16 evenly spaced intervals, and the 9 elements of the  $3 \times 3$  non-handed Mueller matrix are determined from the Fourier transform of those signals.

Bidirectional ellipsometric measurements for samples with various particle sizes will be presented in terms of the principle angle of polarization,  $\eta^{(p)}$ , and the degree of linear polarization,  $P_L^{(p)}$ , as functions of  $\phi_s$  for fixed  $\theta_i$  and  $\theta_s$  for  $p$ -polarized incident light. The laser beam spot size on the sample is about 1 mm in diameter. The surface density of the spheres is about 23000 spheres/mm<sup>2</sup> for the samples containing 181.0 nm and 217.7 nm particles, and 160000 spheres/mm<sup>2</sup> for the 100.7 nm particles. The random measurement uncertainties associated with  $\eta^{(p)}$  and  $P_L^{(p)}$  are estimated by Monte Carlo sampling over a Gaussian distribution about each measured mean value in the  $(\omega, 4\omega)$  scheme with a width given by the respectively measured standard deviation. The uncertainties shown with the data represent the standard deviation of the resulting distributions for  $\eta^{(p)}$  and  $P_L^{(p)}$ . Other systematic sources of uncertainty may exist but are not expected to exceed 2° and 0.05 for  $\eta^{(p)}$  and  $P_L^{(p)}$ , respectively, for most of the range of data.

## 4. RESULTS AND DISCUSSION

Bidirectional ellipsometric measurements were performed on three samples with PSL spheres of diameters 100.7, 181.0 and 217.7 nm on the bare silicon substrate. Measurements for each sample were carried out for  $\theta_i$  and  $\theta_s = 30^\circ, 45^\circ, 50^\circ,$  and  $60^\circ$  at  $\lambda = 532$  nm. Additional measurements at different locations on the wafer were also carried out to study the particle density distribution in the  $\theta_i = \theta_s = 45^\circ$  geometry. As an indication of the relative scattering levels of these three samples and a bare silicon wafer, the bidirectional reflectance distribution functions (BRDF) were also measured. The BRDF levels in the  $\theta_i = \theta_s = 45^\circ$  and  $\phi_s = 90^\circ$  configuration were approximately  $1 \times 10^{-4}$  sr<sup>-1</sup>,  $2 \times 10^{-5}$  sr<sup>-1</sup>,  $4 \times 10^{-6}$  sr<sup>-1</sup>, and  $1 \times 10^{-7}$  sr<sup>-1</sup>, for samples with 217.7 nm spheres, with 181.0 nm spheres, with 100.7 nm spheres, and the bare silicon wafer, respectively. These BRDF results

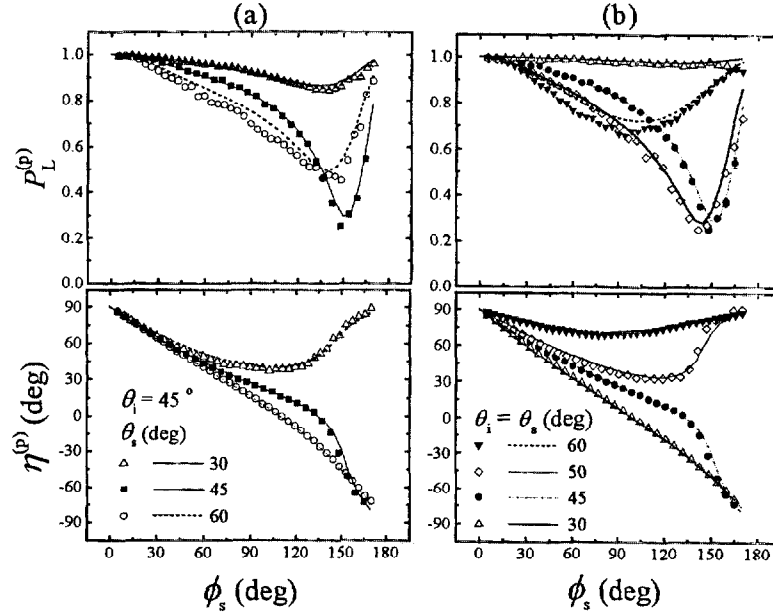


**Figure 5** Bidirectional ellipsometry parameters for 181.0 nm PSL spheres silicon at different incident and scattering angles: (a).  $\theta_i = 45^\circ$ , and  $\theta_s = 60^\circ, 45^\circ$ , and  $30^\circ$ ; (b).  $\theta_i = \theta_s = 60^\circ, 50^\circ, 45^\circ$ , and  $30^\circ$ . The curves represent the predictions of the DDA model. The uncertainties in the data are smaller or about the same size as the symbols.

indicate the scattered intensity from the PSL spheres is at least forty times stronger than that from the bare substrate.

Figure 5 shows the bidirectional ellipsometry parameters for the sample with 181.0 nm PSL spheres as functions of  $\phi_s$  for different values of  $\theta_i$  and  $\theta_s$ . The corresponding theoretical predictions for these bidirectional ellipsometry parameters are presented by the curves indicated in the legend. The experimental data agree very well with the theoretical predictions for all values of  $\phi_s$  at all scattering conditions. A more detailed examination of the data indicates that there is a slight deviation for large  $\theta_i$  or  $\theta_s$ . The differences between the data and the theory for large  $\theta_i$  or  $\theta_s$  may due to the contributions from the interactions between particles, or some existing non-spherical particles on the surface, or because of interference with another scattering mechanisms.

Figure 6 shows the bidirectional ellipsometry results at  $\theta_i = \theta_s = 45^\circ$  for samples with three different diameters. The curves represent the results of the DDA calculations. The theory predicts the overall feature of the angular dependence of the bidirectional ellipsometry parameters for particles with different diameters. We also extract the values of the initial slope,  $-\delta\eta^{(p)}/\delta\phi_s$ , as  $\phi_s \rightarrow 0$ , and present the results with the theoretical predictions in Fig. 4(b). The uncertainties of  $-\delta\eta^{(p)}/\delta\phi_s$  were evaluated by a standard statistical data analysis from the linear regression of the first few data in the  $\eta^{(p)}$  vs.  $\phi_s$  plot (see Fig. 6) and represent at 95 % confidence level. The measured  $-\delta\eta^{(p)}/\delta\phi_s$  values are in good agreement with the theory. This result implies that we indeed can determine the size of the spheres using bidirectional ellipsometric measurements.

The agreement between the measured polarization angles  $\eta^{(p)}$  and those predicted by the theory for 217.7 nm PSL sphere is excellent. However, the corresponding values of measured  $P_L^{(p)}$  are smaller than those predicted

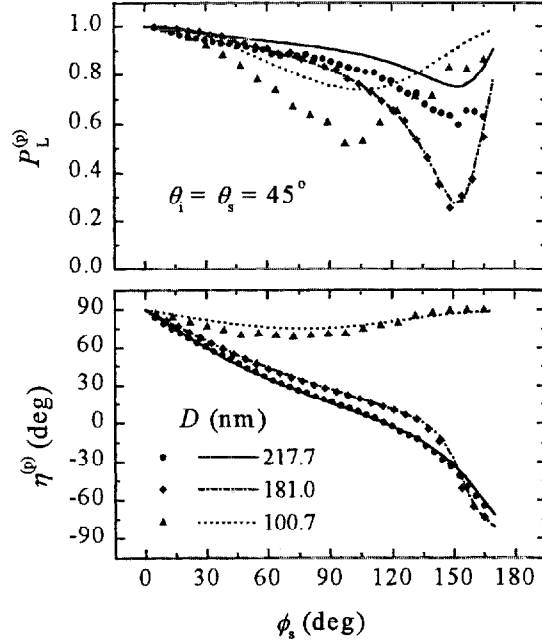


**Figure 6** Bidirectional ellipsometry parameters for three different sizes of PSL spheres on silicon at  $\theta_i = \theta_s = 45^\circ$ . The curves represent the predictions of the DDA model. The uncertainties in the data are smaller or about the same size as the symbols.

by the theory at large scattering angles. The increasing depolarization of light may be occurring because of the growing contribution of minority mechanisms, such as for subsurface defects or microroughness. To examine this possible cause, we conducted bidirectional ellipsometric measurements on the surface far away from the center of the deposition. The selected area has a very few particles, and the result should only reflect the light scattered from the background dominated by surface microroughness and subsurface defects. The BRDF level in the  $\theta_i = \theta_s = 45^\circ$  and  $\phi_s = 90^\circ$  configuration for this area is about  $1 \times 10^{-6} \text{ sr}^{-1}$ , which is about ten times higher than that of a clean silicon wafer. The  $\phi_s$  dependence of  $\eta^{(p)}$  and  $P_L^{(p)}$  agrees with a subsurface defect model, with a highly depolarized light ( $P_L^{(p)} \geq 0.5$ ) for large  $\phi_s$ .

The discrepancy between the data and theory, especially the  $P_L^{(p)}$  data in Fig. 6, for the sample containing 100.7 nm PSL spheres is probably due to the contribution from the doublet particles on the surface. We calculate the bidirectional ellipsometry parameters for a system with two touching 100.7 nm diameter spheres, aligned along the plane of incidence, and perpendicular to the plane of incidence directions. We find the values of  $-\delta\eta^{(p)}/\delta\phi_s$  for these systems to be about 1.3 times, and 2.0 times larger, respectively, than that from a system with a single sphere of 100.7 nm. Without accurate information about the particle density and the geometrical configurations of the doublets, it is difficult to further refine the model to account for the presence of doublets. Further work will be carried out to reduce the fraction of such doublets.

## 5. SUMMARY

Bidirectional ellipsometric measurements of a model system containing well-calibrated polystyrene latex spheres on silicon were made and compared to a discrete dipole approximation model for a sphere above a

smooth surface. The experimental results show good agreement with the theory for this system. This study also demonstrates that the polarization of light scattered by particles can be used to estimate the size of particulate contaminants on a smooth surface.

## ACKNOWLEDGEMENTS

The authors would like to thank Dr. John Small for the field emission scanning microscopy measurements, and to thank Mr. Marco Fernandez for assisting the particle deposition and associated measurements.

## REFERENCES

- <sup>1</sup>T. A. Germer, "Angular Dependence and Polarization of Out-of-plane Optical Scattering from Particulate Contamination, Subsurface Defects, and Surface Microroughness," *Appl. Opt.* **36**, 8798 (1997).
- <sup>2</sup>T. A. Germer, and C. C. Asmail, "Bidirectional Ellipsometry and Its Application to the Characterization of Surfaces," in *Polarization: Measurement, Analysis, and Remote Sensing*, D. H. Goldstein, and R. A. Chipman, ed., Proc. SPIE **3121**, 173 (1997).
- <sup>3</sup>T. A. Germer, C. C. Asmail, and B. W. Scheer, "Polarization of Out-of-plane Scattering from Microrough Silicon," *Opt. Lett.* **22**, 1284 (1997).
- <sup>4</sup>T. A. Germer, and C. C. Asmail, "A Goniometric Optical Scatter Instrument for Bidirectional Reflectance Distribution Function Measurements with Out-of-plane and Polarimetry Capabilities," in *Scattering and Surface Roughness*, Z.-H. Gu, and A. A. Maradudin, ed., Proc. SPIE **3141**, 220 (1997).
- <sup>5</sup>H. C. van de Hulst, *Light Scattering by Small Particles* (Dover, New York, 1981).
- <sup>6</sup>F.C. Bohren and D. R. Huffman, *Absorption and Scattering of Light by Small Particles* (Wiley, New York, 1983).
- <sup>7</sup>G. Videen, "Light Scattering from a Sphere on or Near a Surface," *J. Opt. Soc. Am.* **A8**, 483 (1991); "Errata," *J. Opt. Soc. Am.* **A9**, 844 (1992).
- <sup>8</sup>M. Born and E. Wolf, *Principles of Optics* (Plenum, New York, 1970).
- <sup>9</sup>P. A. Bobbert, and J. Vlieger, "Light Scattering by a Sphere on a Substrate," *Physica A* **137**, 209 (1986).
- <sup>10</sup>B. R. Johnson, "Calculation of Light Scattering from a Spherical Particle on a Surface by the Multipole Expansion Method," *J. Opt. Soc. Am.* **A13** 326 (1996).
- <sup>11</sup>W. S. Bickel, A. J. Watkins, and G. Videen, "The Light Scattering Mueller Matrix Elements for Rayleigh, Rayleigh-Gans, and Mie Spheres," *Am. J. Phys.* **55**, 559 (1987).
- <sup>12</sup>G. Videen, W. L. Wolfe and W. S. Bickel, "Light Scattering Mueller Matrix for a Surface Contaminated by a Single Particle in the Raleigh Limit," *Opt. Eng.* **31**, 341 (1992).
- <sup>13</sup>D. S. Flynn, and C. Alexander, "Polarized Surface Scattering Expressed in Terms of a Bidirectional Reflectance Distribution Function Matrix," *Opt. Eng.* **34**, 1646 (1995).

- <sup>14</sup>R. Schmehl, B. M. Nebeker, and E. D. Hirleman, "Discret-Dipole Approximation for Scattering by Features on Surfaces by Means of a Two-dimensional Fast Fourier Transform Technique," *J. Opt. Soc. Am.* **A14**, 3026 (1997).
- <sup>15</sup>G. W. Starr and E. D. Hirleman, "Comparison of Experimentally Measured Differential Scattering Cross Sections of PSL Spheres on Flat Surfaces and Patterned Surfaces," in *Flatness, Roughness, and Discrete Defect Characterization for Computer Disks, Wafers, and Flat Panel Displays*, J. C. Stover, ed., Proc. SPIE **2862**, 130 (1996).
- <sup>16</sup>B. M. Nebeker, G. W. Starr, and E. D. Hirleman, "Modeling of Light Scattering from Structures with Particle Contaminants," in *Flatness, Roughness, and Discrete Defect Characterization for Computer Disks, Wafers, and Flat Panel Displays*, J. C. Stover, ed., Proc. SPIE **2862**, 139 (1996).
- <sup>17</sup>S. V. Hering, R. C. Flagan, and S. K. Friedlander, "Design and Evaluation of a New Low-Pressure Impactor. 1," *Env. Sci. Technol.* **12**, 667 (1978).
- <sup>18</sup>S. V. Hering, S. K. Friedlander, J. J. Collins, and L. W. Richards, "Design and Evaluation of a New Low-Pressure Impactor. 2," *Env. Sci. Technol.* **13**, 184 (1979).
- <sup>19</sup>P. D. Kinney, D. Y. H. Pui, G. W. Mulholland, and N. P. Bryner, "Use of the Electrostatic Classification Method to Size 0.1  $\mu\text{m}$  SRM Particles - A Feasibility Study," *J. Res. Natl. Inst. Stand. Technol.* **96**, 147 (1991).
- <sup>20</sup>The reference to commercial equipment or product does not imply its recommendation or endorsement by National Institute of Standards and Technology.
- <sup>21</sup>G. W. Mulholland, N. Bryner, W. Liggett, B. W. Scheer, and R. K. Goodall, "Selection of Calibration Particles for Scanning Surface Inspection System," in *Flatness, Roughness, and Discrete Defect Characterization for Computer Disks, Wafers, and Flat Panel Displays*, J. C. Stover, ed., Proc. SPIE **2826**, 104 (1996).
- <sup>22</sup>G. W. Mulholland and M. Fernandez, "Accurate Size Measurement of Monosize Calibration Spheres by Differential Mobility Analysis," in *Characterization and Metrology for ULSI Technology*, Seiler et al., ed., Proc. AIP **449**, 819 (1998).
- <sup>23</sup>G. W. Mulholland, N. P. Bryner, and C. Croarkin, "Measurement of 100 nm NIST SRM 1963 by Differential Mobility Analysis," submitted to *J. Aerosol Sci. and Technol.* (1998).
- <sup>24</sup>C. C. Asmail, C. L. Cromer, J. E. Proctor, and J. J. Hsia, "Instrumentation at National Institute of Standards and Technology for bidirectional Reflectance distribution Function (BRDF) Measurements," in *Stray Radiation in Optical System III*, R. P. Breault, ed., Proc. SPIE **2260**, 52 (1994).
- <sup>25</sup>R. M. A. Azzam, "Photopolarimetric Measurement of Mueller Matrix by Fourier Analysis of a Single Detected Signal," *Opt. Lett.* **2**, 148 (1978).